Conf-920430--87

PNL-SA--19999

DE92 012337

EXPERIMENTAL CHARACTERIZATION OF JET FORCES ON WASTE TANK COMPONENTS

J. A. Bamberger
J. M. Bates
E. D. Waters

Received by OSTI
APR 28 1992

April 1992

Presented at the
American Nuclear Society International High Level Radioactive Waste Management
April 12-16, 1992
Las Vegas, Nevada

Work supported by
the U.S. Department of Energy
under Contract DE-AC06-76RLO 1830

Pacific Northwest Laboratory
Richland, Washington 99352

DISCLAIMER

This report was prepared as an account of work sponsored by an agency of the United States Government. Neither the United States Government nor any agency thereof, nor any of their employees, makes any warranty, express or implied, or assumes any legal liability or responsibility for the accuracy, completeness, or usefulness of any information, apparatus, product, or process disclosed, or represents that its use would not infringe privately owned rights. Reference herein to any specific commercial product, process, or service by trade name, trademark, manufacturer, or otherwise does not necessarily constitute or imply its endorsement, recommendation, or favoring by the United States Government or any agency thereof. The views and opinions of authors expressed herein do not necessarily state or reflect those of the United States Government or any agency thereof.

MASTER

DISTRIBUTION OF THIS DOCUMENT IS UNLIMITED

EXPERIMENTAL CHARACTERIZATION OF JET FORCES ON WASTE TANK COMPONENTS

Ms. Judith Ann Bamberger, P.E.
Pacific Northwest Laboratory
P. O. Box 999
Richland, Washington 99352
(509) 375-3898

Mr. James M. Bates, P.E.
Pacific Northwest Laboratory
P. O. Box 999
Richland, Washington 99352
(509) 375-2539

Mr. E. Dale Waters, P.E.
Westinghouse Hanford
P. O. Box 1970
Richland, Washington 99352
(509) 373-5304

ABSTRACT

Scaled experiments were performed to characterize the forces of fluid jets impacting waste tank components. The fluid jets will be produced by mixer pumps used to resuspend settled solids in million-gallon burried waste tanks on the Hanford site. Components (including a radiation dry well, air lift circulator, and steam coil) were modeled at 1/6-scale. Forces on the full-scale tank components are predicted based on experimental data and theoretical scaling relationships. Drag coefficients, determined for the radiation dry well and air lift circulator, were used to develop relationships between fluid jet parameters and the impact forces on these two components.

INTRODUCTION

Radioactive wastes, stored in million-gallon double-shell tanks (DSTs), are to be retrieved as part of the overall cleanup of the U.S. Department of Energy's Hanford Site in southeastern Washington. The DST wastes generally consist of a liquid supernatant over a much smaller volume of settled solids. The current reference approach is to resuspend the settled solids with mixer pumps located near the tank floor. These pumps will generate two horizontal, opposed, high-volume, high-velocity jets of tank fluid and direct the jets at the settled solids. As the pump slowly oscillates, the jets sweep out arcs of fluid that suspend and mix the settled solids with the waste fluid. Some tanks contain internal components, suspended from the dome, that extend into the path of the expanding jets. There is concern that the impact forces of the jets may damage internal components. To address this concern an analysis was performed to define the non-uniform nature of the near-floor jet velocity profiles and their interactions with the complex geometries of the structures in the path of the jet. Experiments were conducted to quantify the impact forces for three tank components. These forces are presented based on two approaches: 1) measured data are scaled to the force on waste tank components using theoretical scaling relationships, and 2) correlations of force on waste tank components are developed based on experimentally determined effective drag coefficients and jet velocity profiles.

THEORETICAL BACKGROUND

This experimental study, based on hydraulic force similarity between a 1/6-scale model and the prototype [75-ft diameter, million-gallon tanks at Hanford], was designed to satisfy geometric, kinematic, and fluid dynamic ratios. A diagram of the experimental model is shown in Figure 1. The potential effects of nearby solid boundaries, such as the tank floor and the test articles, are similar in the model and prototype. Geometric scaling is applied to four ratios 1) the elevation of the jet nozzle above the floor (E) to the jet diameter (d_{jet}), 2) the ratio of the test article diameter (d_{cyl}) to jet diameter, 3) the ratio of cylinder offset from the nozzle centerline (off_{cyl}) to the jet diameter, and 4) the ratio of test article diameter to the nozzle diameter (d_o).

A. Submerged Jet Fluid Dynamic Scaling

A submerged jet, discharged through a nozzle, can be characterized by three regions: 1) an irrotational core, wherein the jet centerline velocity equals the nozzle exit velocity; 2) a transition region; and 3) a mixing region where the jet flow is fully established and the jet diameter expands at a relatively constant angle. The mixing region is the area of interest to this study. The velocity (U) at any point within the established, submerged, free jet (assuming no interaction with a component or waste tank floor or wall) is a function of the jet half angle of expansion (Θ), the normalized distance from the nozzle (x/d_o), and the radial distance from the jet centerline (r).

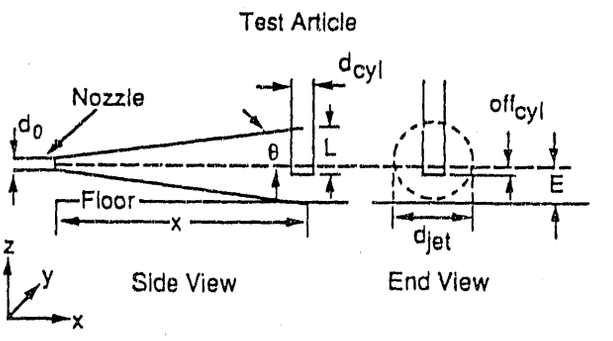

Figure 1. Model Diagram

This can be expressed as

$$U = f(U_o, x/d_o, \Theta, r) \quad (1)$$

where U_o is nozzle exit velocity.

An empirical mathematical expression relating the jet half angle of expansion (the angle measured from the cone surface to the cone axis, determined photographically) and the kinematic viscosity of the jet fluid was observed by Donald and Singer as

$$\tan \Theta = 0.238\ \nu^{0.133} \quad (2)$$

where ν is the fluid kinematic viscosity in Stokes (1 Stoke = 1.076×10^{-3} ft^2/s).[1] The relationship was deduced using data from four Newtonian fluids: water, sugar solution, air, and hydrogen flowing into air. Kinematic viscosities of these four fluids range from 1.07×10^{-5} to 1.07×10^{-3} ft^2/s. Therefore, the relationship should be valid to quantify the jet angle of expansion of the prototype waste tank slurry ($\nu = 1.79 \times 10^{-5}$ ft^2/s, assumed Newtonian because of the high water content) and the model fluid, water ($\nu = 6.58 \times 10^{-6}$ ft^2/s at 111 F).

In the mixing region, beyond the point where the jet flow is fully established, the centerline velocity [$U_c(x)$] of a free jet can be calculated as a function of distance (x) from the nozzle by the equation

$$U_c(x)/U_o = K\, d_o/x \quad (3)$$

where K is the diffusion coefficient.[2] Once the modeling scale is selected and the fluid properties are known, the axial distance relationship between model and prototype is established using Equations (2) and (3).

Finally, it is assumed that dynamic similarity exists when the Reynolds number (Re) of the model component equals that of the prototype component at the scaled location (x). Reynolds number scaling is based on the jet centerline velocity for a free jet as a function of the distance from the nozzle [$U_c(x)$] and the diameter of the test article.

$$Re_m = [(U_c(x)\, d_{cyl}\, \rho)/\mu]_m = Re_p = [(U_c(x)\, d_{cyl}\, \rho)/\mu]_p \quad (4)$$

The velocity, fluid density (ρ) and viscosity (μ) were adjusted for the test to make the model (m) and prototype (p) Reynolds numbers equal and satisfy Equation (4).

B. Impact Force Scaling

Fluid impingement on the component by the jet creates a pressure force, normal to the surface and a frictional force, tangential to the surface, which resolve into the drag component (F_d) parallel to the initial flow stream, and lift component (F_l) perpendicular to the fluid motion. Drag and lift forces are considered independently.

Drag coefficient (C_d) is defined in terms of the drag force

$$C_d = F_d/(\rho\, A\, U^2/2) \quad (5)$$

where U is free stream fluid velocity and A is profile area. C_d is made up of two terms:

$$C_d = C_p + C_f\, A_s/A \quad (6)$$

where C_p is pressure coefficient, C_f is skin-friction coefficient, and A_s is characteristic surface area for shear. For cylinders in a uniform crossflow field, more than 90% of the drag is caused by pressure variation while less than 10% results from viscous stresses on the surface. For these conditions, it has been found that the drag coefficient decreases significantly as the Reynolds number increases from 10^5 to 10^6.[3] This reduction is attributed to the increased turbulence present in the fluid boundary layer. The drag coefficient is also a function of the surface roughness (ϵ/d_{cyl}) and the free stream turbulence (TI), parameters that affect the boundary layer separation mechanism. Literature data are not consistent with respect to the quantitative effects of free stream turbulence or its effect upon drag coefficient.[4] Even so, in this analysis the drag coefficient is assumed to be a function of Reynolds number, characteristic area, surface roughness, and turbulence intensity, expressed as

$$C_d = f(Re, d_{cyl}, L, \epsilon/d_{cyl}, TI) \quad (7)$$

where L is length of the test article impacted by the jet.

Using Equation (5) to characterize the drag force, the ratio of the drag forces between the prototype (F_p) and the model (F_m) is

$$F_p/F_m = (C_{dp}\, \rho_p\, U_p^2\, A_p)/(C_{dm}\, \rho_m\, U_m^2\, A_m) \quad (8)$$

Equation (8) will be used to scale the impact force on the prototype from measurements of the force on the model by equating the drag coefficients of the model and the prototype. The scaling relationships are 1) fluid properties for the prototype (ρ_p = 74.914 lbm/ft^3) are known at the design point; 2) fluid properties for the model (ρ_m = 61.8467 lbm/ft^3) are a function of the fluid temperature measured during the experiment; 3) test article dimensions are scaled (A_p/A_m = 36); 4) the model jet velocity profile is scaled geometrically and dynamically. The Reynolds number equivalence relationship, Equation (4), relates the velocities (U_p^2/U_m^2 = 0.1581); 5) the surface roughness is of only minor importance and is scaled; and 6) the turbulence intensities in the model and prototype are not scaled.[5] However, the flow will be highly turbulent in both the model and the prototype. Based on the experiment scale and operating conditions Equation (8) then reduces to

$$F_p = 6.89\, F_m \quad (9)$$

Thus, the jet impact force on a prototype waste tank component is projected to be 6.89 times the force on the model component at a scaled axial distance (x) from a nozzle with the scaled nozzle discharge parameter ($U_o d_o$) used in these tests.

EXPERIMENTAL ARRANGEMENT

A schematic diagram of the facility is shown in Figure 2. The jet nozzle, located at a fixed position near the tank wall parallel to the floor and perpendicular to the tank wall, was directed toward the center of the tank. The experiments were conducted in an existing 6-ft diameter, 9-ft high tank. Although the test tank dimensions do not correspond to a 1/6-scale of the full scale DST, they match reasonably well with the nozzle-to-wall dimensions of a single liquid jet located at the center of a DST. Also, other arrangements were provided to scale the DST dimensions. To model liquid depth, the tank was partitioned into two regions by a false floor, 3-ft from the tank upper rim. This floor was used to regulate bulk flow circulation patterns and limit vertical length of model components. At the tank wall directly opposite the nozzle, turning vanes direct the jet flow to the lower portion of the tank. An annular space, sized to limit velocities to <3 ft/s around the edge of the false floor, allowed fluid to flow from the lower section of the tank for flow entrainment into the expanding jet.

Test articles were suspended from a test frame on top of the tank (Figure 3). Tension/compression load cells were used to measure the axial and lateral forces on the test articles. Test articles positions were monitored using a translation stage (elevation was manually positioned). A turbine flowmeter on the pump suction line was used to monitor flow rate. Instrumentation and measurement accuracy are summarized in Table 1.

A. Test Articles

Jet forces were evaluated for models of a radiation dry well, air lift circulator, and steam coil, shown in Figure 4. The dimensions for the scaled test articles are summarized in Table 2. These items were constructed to geometrically match waste tank components in the jet path according to design drawings at a 1:6 scale ratio of model to prototype.

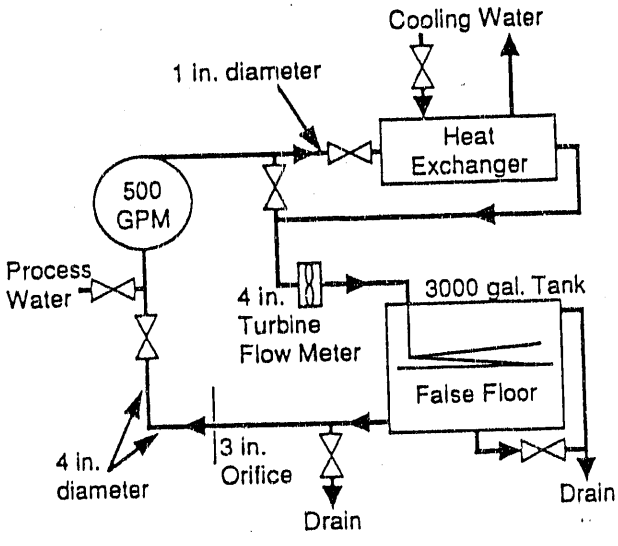

Figure 2. Experimental Facility Flow Diagram

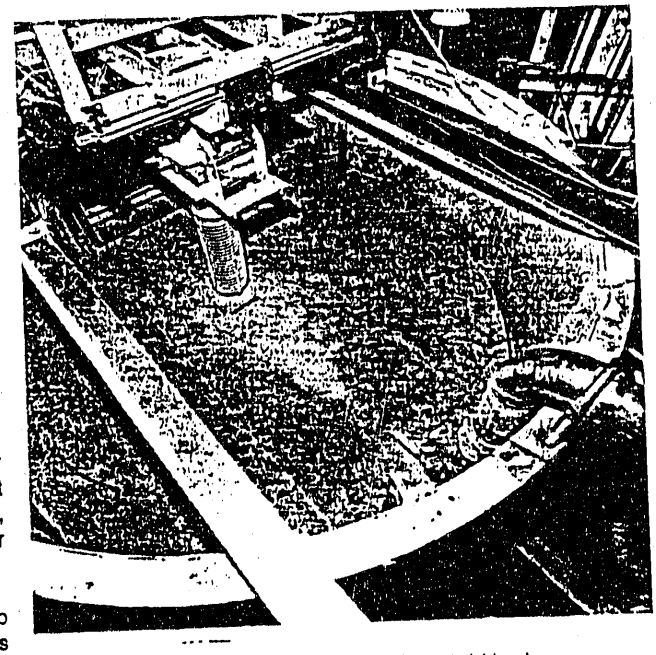

Figure 3. Test Facility and Experimental Hardware

Table 1. Instrumentation and Accuracy

Measured Variable	Measurement Instrument	Accuracy
temperature	thermocouple	±1.0 F
flow rate	turbine flowmeter	±0.5%
velocity	differential pressure transducer	±3.8 ft/s
test position	linear variable displacement transformer	±0.075 in.
axial force	load cell	±1.15 lbf
transverse force	load cell	±0.12 lbf

The radiation dry well model is a right circular, solid aluminum cylinder. The model extends 2-1/2 in. below the nozzle centerline and intersects the expanding liquid jet at all scaled distances from the nozzle.

The air lift circulator model is a right circular cylinder, with the lower end open. It extends to a position 2 in. above the nozzle centerline. Forces on the air lift circulator are asymmetric because of a cylindrical thermocouple guide extending along the side of the cylinder to 2-1/2 in. below the nozzle centerline. It is positioned at the air lift circulator perimeter. All experiments were conducted with the thermocouple guide

Table 2. Test Article Dimensions

Test Article	Article Dimensions and Tolerances
nozzle	circular, 1.0 in. diameter ±0.001 in.
radiation dry well	cylinder (solid), 1.104 in. diameter ±0.005 in.
air lift circulator (ALC)	cylinder, wall thickness 0.125, 5.000 in. outside diameter, ±0.005 in.
ALC guide	cylinder (solid), 0.175 in. diameter ±0.005 in.
steam coil	three coiled cylinders, 6.729-in. maximum diameter, 3.485-, 5.000-, 6.501-in. helix diameters ±0.01 in., 0.667 in. staggered pitch. I-beam support framework.

centered at the leading edge of the circulator, conservatively positioned to receive the maximum force.

The steam coil model consists of three concentric helical coils supported by two central vertical I-beams and a lower horizontal support I-beam. The steam coil model physically represents the major components of the steam coil that provide the main source of the component drag within the jet; minor details were not modeled. The major sources of steam coil drag are the coils and the horizontal and vertical I-beams. Forces impacting the steam coil may be asymmetric because of the lower horizontal I-beam orientation. The steam coil was tested at two elevations (vertical locations): 3 in. and 9 in. above the tank floor. The steam coil was impacted by the jet at all 3-in. elevation positions, but had little or no interaction with the jet at 9-in. elevations.

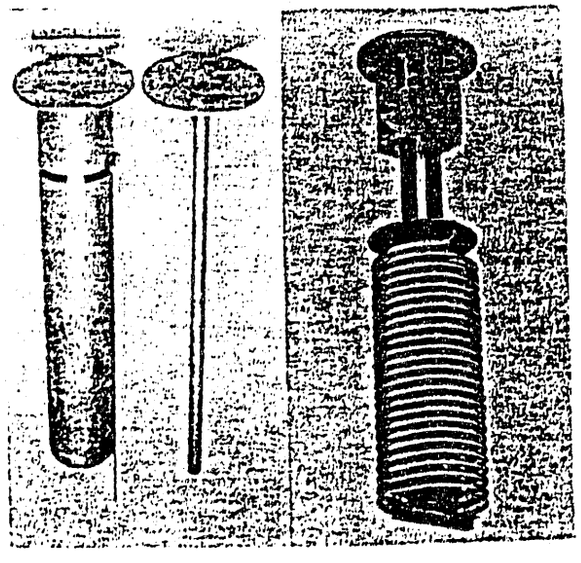

Figure 4. Model of Air Lift Circulator with Thermocouple Guide, Radiation Dry Well, and Steam Coil (left to right)

B. Experimental Procedure

To obtain a test condition the axial distance from the nozzle (x) and the vertical elevation (z) were established; the flow rate was set and fluid temperature confirmed; then measurements were taken at varying transverse positions (y) across the jet. The test article location matrices for model and corresponding prototype locations are listed in Table 3. Test conditions are summarized in Table 4.

Table 3. Prototype and 1/6-Scale Model Experimental Configurations[a]

Test Article	Elev. from Floor to Nozzle Center-line, in.	Elev. from Floor to Test Article, in.	Distance from Test Article to Nozzle[b] ft (in.)
Radiation dry well	18 (3)	3 (0.5)	5 (11) 11 (25) 18 (41) 25 (57)
Air lift circulator	18 (3)	30 (5)	5 (11) 11 (25) 18 (41) 25 (57)
Steam coil[c]	12 (2)	18 (3)	14.6 (33.5) 25 (57)
	18 (3)	18 (3)	14.6 (33.5) 25 (57)
	18 (3)	54 (9)	14.6 (33.5) 25 (57)

(a) Model values are shown in parenthesis.
(b) The prototype nozzle exit is 17.5 in. from the pump centerline.
(c) Three I-beam orientations--parallel, perpendicular, and 45-degree angle to the flow--were evaluated at nozzle exit velocity U1. At nozzle exit velocities U2, U3, and U4 the force measurements were only taken with the I-beam perpendicular to the flow.

Table 4. Prototype[a] and Model[b] Operating Conditions

Case I.D. Number	Exit Velocity ft/s Prototype	Exit Velocity ft/s Model
U1	58.8	147.92
U2	45.0	113.20
U3	30.0	75.47
U4	15.0	37.73

(a) Prototype, full-scale, 6-in.-diameter nozzle, slurry at 220 F with ρ=74.914 lbm/ft^3 and μ=1.3439x10^{-3} lbm/ft-s.
(b) Model, 1/6-scale, 1.00-in.-diameter nozzle, water at 111 F with ρ=61.8467 lbm/ft^3 and μ=4.0717x10^{-4} lbm/ft-s.

RESULTS AND DISCUSSION

A. Measured Forces

The drag forces on the waste tank prototype components were calculated from the time-averaged (10 sec average) model measured forces using Equation (9) and are summarized in Table 5.

Table 5. Scaled Forces on Prototype DST Equipment

Axial Dist. ft	Case I.D. Number	Calculated Force[a], lbf: Radiation Dry Well	Air Lift Circulator	Steam Coil[b]
3.6	U1		89[c]	
5	U1		83	
	U2		55	
	U3		27	
	U4		5.5	
7	U1		113[c]	
11	U1	167	94	
	U2	91	54	
	U3	38	24	
14.4	U2-per[d]			180
	U3-per			84
	U4-per			21
14.6	U1-par			115
	U1-45			233
	U1-per			303
18	U1	79	71	
	U2	45	43	
25	U1-par	47	55	66
	U1-45			113
	U1-per			164
	U2-per			97
	U3-per			43
	U4-per			10
37.4	U1-per			109 [c]
	U2-per			80 [c]
	U3-per			43 [c]

(a) Equivalent force applied to lower end of test article.
(b) At 18-in. elevation above DST floor.
(c) Extrapolated from experimental data points.
(d) Orientation of steam coil horizontal I-beam to the jet flow are described by per = perpendicular, 45 = 45 degrees, and par = parallel.

B. Drag Coefficients

The experimentally measured force and jet velocity profile data were evaluated to develop values of drag coefficients.[5] In this analysis, there were two concerns: 1) the development of drag coefficients for a non-uniform flow field, and 2) the potential of wide variation in drag coefficient for very minor changes in Reynolds number, effects which could complicate development of drag force correlations.

Equation (5) can be applied to the jet force experiment model if several important assumptions and limitations are realized. Drag coefficients for three-dimensional bodies are typically defined for the case where that body is subjected to a uniform flow field, with the Reynolds number essentially constant over the length of the body. For a submerged liquid jet, the assumption of uniform velocity is unattainable if the characteristic dimensions of the drag body are significant compared to the dimensions of the jet structure as in the case for this study.

The distribution of forces over the length of the model is required to calculate an accurate drag coefficient for the test articles. However, only the total force was measured in the tests. Thus, an approximation of the fluid velocity distribution impacting the model is required.

Radiation Dry Well. The narrow model width in comparison to the jet horizontal profile width allows for good approximation of the local jet velocity using only the measured vertical velocity profile at the jet centerline. Averages of the jet velocity over that vertical zone impacting the dry well model were calculated by two differing techniques: 1) the average impact velocity was calculated as a linear average over the height of the vertical velocity profile with the center of applied force assumed at the jet centerline, and 2) an averaging technique was used wherein the centroid of the velocity profile was calculated to determine the center of applied drag force and the area weighted average velocity was determined. For each technique an effective drag coefficient was calculated using the average velocity, the measured force and Equation (5). To compare these calculated drag coefficients with generally accepted values for cylindrical bodies, Reynolds number values for each method are listed in Table 6. Examination of the calculated drag coefficients reveals a reasonable range of values when compared to those generally accepted, especially in light of the rather subjective techniques used to arrive at average velocity values.[3]

A more general approach to drag coefficient characterization was investigated wherein a parameter termed the effective drag coefficient (C_e) was calculated from the model data using the following relationship:

$$C_e = F_m/(\rho_m U_{max,m}^2) \qquad (10)$$

where $U_{max,m}$ is the maximum model jet velocity for a near-floor jet. This C_e term incorporates the impact area of the jet on the test article. For the radiation dry well data, C_e appeared to exhibit dependence on U_{om} and a relation for C_e was formulated:

$$C_e = 0.0011\ U_{om}^{0.412} \qquad (11)$$

For the radiation dry well model, this relation yields values within $\pm$10% of those calculated by use of Equation (10) for each test condition data set.

Air Lift Circulator. Drag coefficient calculations for this model are complicated by the differing geometry of the body and the guide. With only a total drag force value available, determining the fraction attributable to each component is not straightforward. When the air lift circulator model is located 11 in. from the nozzle, only the thermocouple guide is impacted by the jet, and the drag coefficient analysis should be straightforward. At this axial location, for nozzle exit velocity U1 through U4, the

Table 6. Calculated Drag Coefficients and Reynolds Numbers for Model Radiation Dry Well

Case I.D. Num.	Axial Position x, in.	Reynolds Number (10^5) based on Area	Reynolds Number (10^5) based on Linear	Drag Coefficient based on Area	Drag Coefficient based on Linear
U1	25	4.27	3.53	0.69	1.01
	41	2.72	2.08	0.68	1.12
	57	1.86	1.40	0.72	1.31
U2	25	3.17	2.58	0.67	1.02
	41	2.05	1.54	0.58	1.15
	57	1.49	1.12	0.53	0.98
U3	41	1.36	1.01	0.49	0.91

drag coefficient calculated using Equation (5) ranges from 1.1 to 1.4 for these assumptions. (C_d at U1 = 1.07, C_d at U3 = 1.35).

For the larger axial distances ($x_m \geq 25$ in.) an approach similar to that outlined for the radiation dry well was incorporated to arrive at an effective drag coefficient (C_e). For the air lift circulator with a proportionately larger jet impact area, the effective drag coefficient was found to vary linearly with axial distance such that

$$C_e = 0.0022\, x_m \tag{12}$$

where x_m equals the model axial distance from nozzle (ft). This relation yields effective drag coefficients in agreement with the test data to within $\pm$13%.

Steam Coil. The steam coil presents a geometry even more complex than the air lift circulator, further complicating the evaluation of effective drag coefficients because of the lack of information on the distribution of drag forces among the various separate components of the assembly. One approach used to examine the force data was to assume that when the lower I-beam support is parallel to the jet axis, its drag contribution is negligible, and to assume that all forces are generated from the coils. In this approach the coils are modeled as a simple solid cylinder with an outside diameter equal to that of the outermost coil. Then when the I-beam is not parallel to the jet axis, the I-beam drag force is taken as the difference in force measured between the parallel and perpendicular orientations.

At nozzle exit velocity U1, 57 in. from the nozzle, the effective C_d for the coil section was calculated to be 0.91, typical of cylindrical drag bodies. At this same location and Reynolds number a C_d of 2.13 was calculated for the I-beam support in the perpendicular, maximum drag orientation. This value is typical of published values for similar geometries such as square rods in cross flow and rectangular flat plates perpendicular to the flow.[3]

An effective drag coefficient for the steam coil was calculated using Equation (10) and the limited data available for the steam coil in the I-beam perpendicular orientation. For this data set, C_e = 0.0247 resulted in matching all individually calculated F_m values to within $\pm$24%. With this range of uncertainty and limited data set, no general correlation is presented. These approaches to steam coil drag coefficient derivation seem to yield reasonable results.

C. Force Correlations

Force correlations for the radiation dry well and the air lift circulator are presented as a function of component centerline distance from the nozzle exit and the nozzle discharge parameters. Information is presented from two approaches: 1) data points were obtained by scaling model force measurements to prototype conditions using Equation (9), and 2) curves were obtained by using equivalent drag coefficient correlations and velocity profile correlations to calculate prototype forces.[5]

Radiation Dry Well. A relation was developed describing the force impacting the prototype as a function of prototype operating parameters. Force on the prototype is defined by Equation (9); force on the model is defined by Equation (10) where C_e is effective drag coefficient;

$$U_{max,m} = K_{3\text{-in.}}\, U_{om}\, d_{om}/x_m \tag{13}$$

where U_{om} is model nozzle exit velocity (ft/s); x_m is distance from nozzle to model centerline (ft); and d_{om} is model nozzle diameter (ft). $K_{3\text{-in.}}$ is obtained from tests with 3 in. floor-to-nozzle centerline spacing and expressed by Equation (13).[5]

$$K_{3\text{-in.}} = [13.86\, U_{om}^{-0.186}]\, [x^{(0.036\, U_{om}^{0.369})}] \tag{14}$$

Location relationships between the model and the prototype parameters are scaled. The prototype axial distances from the nozzle (x_p) are derived as

$$x_p = (x_m\, d_{cyl,p} \tan \theta_m)/(d_{cyl,m} \tan \theta_p) \tag{15}$$

where x_m is the model distance from nozzle (ft). Combining Equations (9), (13), (14), and (15) the axial force (F_p) correlation is

$$F_p = [0.1275\, U_{op}^{2.040}]\, [(x_p/5.252)^{(0.051\, U_{op}^{0.369} - 1)}]^2 \tag{16}$$

where F_p is prototype radiation dry well axial force (lbf), U_{op} is prototype nozzle exit velocity (ft/s), and x_p is prototype axial distance from pump nozzle (ft). The curves shown in Figure 5 are based on Equation (16); the data points are calculated from Equation (9) using measured model forces. Calculated values of F_p check within $\pm$6 lbf of prototype values scaled from test measurements. Equation (16) is thus recommended for use in calculating prototype radiation dry well force. Extrapolation of the above relationships to axial distances or nozzle flow rates and/or sizes beyond those modeled in the current effort should be attempted only with caution and after thorough analysis.

Air Lift Circulator. The data, scaled to prototype forces as described for the radiation dry well, are presented in Figure 6 as open data points. At nozzle exit

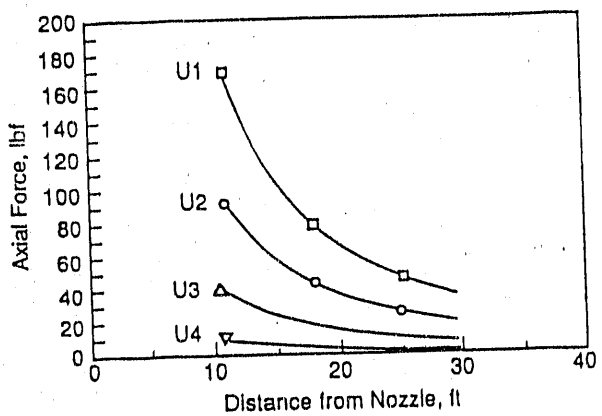

Figure 5. Prototype Radiation Dry Well Force Versus Distance from Nozzle Exit (Comparison of Data and Correlation).

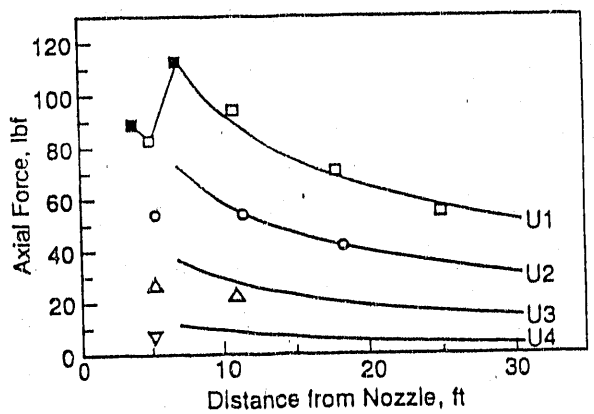

Figure 6. Prototype Air Lift Circulator Force Versus Distance from Nozzle Exit (Comparison of Data and Correlation).

velocity U1, the force on the air lift circulator assembly is greater at 11 ft from the nozzle exit than at 5 ft from the nozzle exit. This results because at the closer distance, the jet passes beneath the body of the air lift circulator and only impacts the thermocouple guide; at the 11 ft distance from the nozzle exit, the jet radius has expanded and is impacting the lower portion of the air lift circulator body as well as the thermocouple guide.

A correlation was developed describing the force impacting the air lift circulator prototype based on prototype operating parameters using the same methodology presented for the radiation dry well. The correlation between prototype nozzle velocity (U_{op}), distance from nozzle (x_p), and axial force (F_p) is applicable for a test range equivalent to 11 ft < x_p < 30 ft and d_{op} = 0.5 ft:

$$F_p = [0.03322\, x_p\, U_{op}^{1.626}]\, [(x_p/5.252)^{(0.051\, U_{op}^{0.369} - 1)}]^2 \qquad (17)$$

Calculated values of F_p from Equation (17) compare to direct scaled values within ±6 lbf. Note that x_p is the prototype distance from the nozzle in ft.

In the waste tank, air lift circulators are located 3.6 and 7.0 ft from the nozzle. No measurements were taken at these distances. The existing force data, force correlation, and air lift circulator geometry were analyzed to estimate the magnitude of the axial force impacting circulators at these two locations. Forces impacting the prototype of 89 lbf at a distance of 3.6 ft and 113 lbf at a distance of 7.0 ft were calculated, respectively.

Figure 6 shows forces on the prototype at distances of 5, 11, 13, and 25 ft from the nozzle as open symbols. The forces are derived from measurements on the model. In addition, forces at nozzle exit velocity U1 were estimated at distances of 3.6 and 7.0 ft from the nozzle and are shown as shaded symbols. A correlation of force versus distance valid for nozzle exit velocity range U1 through U3 [Equation (17)] can be used for prototype distances ≥7 ft from the nozzle exit. Caution should be used for any extrapolation of this correlation beyond the range of actual test conditions.

Steam Coil. Using Equation (9), the measured force values for the model steam coil were scaled to prototype conditions and are presented in Table 5. Steam coil horizontal I-beam configurations ordered by decreasing force are U1-per, U1-45, U2-per, U1-par, U3-per, and U4-per. Facility size limited nozzle to model centerline distances and no data were obtained corresponding to an actual prototype steam coil distance of 37.4 ft from the nozzle exit. Forces (F) were extrapolated to this location. At the test article, the area of impact can be approximated by a rectangle of width (d_{cyl}) and height (r_{jet}) for the model lower edge at the jet centerline, and the jet velocity can be defined as the velocity at the jet centerline. The ratio of centerline velocities reduces to a ratio of distances from the nozzle. Therefore,

$$F_2 = (F_1\, x_1^2\, r_{jet2})/(x_2^2\, r_{jet1}) \qquad (18)$$

where subscript 1 refers to a data location and subscript 2 refers to any other location. Data obtained at either 14.6 or 25 ft from the nozzle were scaled using Equation (18) to estimate the force impacting the steam coil at 37.4 ft from the nozzle exit. Forces obtained at 37.4 ft compared well using either reference point. This confirmed the validity of the extrapolation technique. The average of the two values is listed in Table 5.

No correlations are presented for the steam coil in the raised position, 54 in. above the tank floor, because small forces (<4 lbf) were measured on the model at this elevation, and this would translate to less than 28 lbf on the prototype which would not be significant.

D. Uncertainty

The uncertainty associated with calculating the impact force on the prototype (F_p) is estimated using Equation (8). The uncertainties were determined for the three test articles at nozzle exit velocity U1 at the closest and farthest distances from the nozzle at the jet centerline.

At positions nearest the nozzle where the jet velocity is high, force uncertainties associated with the experimental parameters are $\pm$14%, $\pm$15%, and $\pm$19% for the radiation dry well, air lift circulator, and steam coil, respectively. Most of the force uncertainty associated with the measurements is caused by the uncertainty associated with the jet velocity. In this case, the velocity referred to is the average velocity over the impact area. Uncertainties of the areas of the test articles exposed to the jet are the next dominant terms.

The drag coefficients for the test articles were calculated from the measured loads on the test article using Equation (5). The uncertainty analysis for the drag coefficient is presented for the same range of conditions as the force uncertainty analysis. For the analyses nearest the nozzle, drag coefficient uncertainties ranged from 12% to 15%, 15% to 19%, and 17% to 22% for the radiation dry well, air lift circulator, and steam coil, respectively.

SUMMARY

Static forces on waste tank components produced by mixer pump jets impacting the portion of the component within its path were evaluated via scaled experiments. Forces impacting the prototypes were scaled from the model data. Drag coefficients, derived for the radiation dry well and air lift circulator, agreed well with measured data. Effective drag coefficients were developed to describe the drag for radiation dry wells and air lift circulators as a function of specific range of distances from the jet nozzle to the test article and specific jet Reynolds numbers. These correlations will be used to predict the static forces impacting these components in waste tanks for a range of proposed operating conditions.

ACKNOWLEDGMENTS

This research, conducted by Pacific Northwest Laboratory (operated for the U.S. Department of Energy by Battelle Memorial Institute), was supported by the U.S. Department of Energy under contract DE-AC06-76RLO 1830. The work was sponsored by Westinghouse Hanford Company.

NOMENCLATURE

A	profile area
A_s	characteristic surface area for shear
C_d	drag coefficient
C_e	effective drag coefficient
C_f	skin friction coefficient
C_p	pressure coefficient
d_{cyl}	test article diameter
d_{jet}	jet diameter
d_o	nozzle diameter
E	elevation of jet nozzle above tank floor
F	force
F_d	drag force
F_l	lift force
F_m	drag force on model
F_p	drag force on prototype
K	diffusion coefficient
$K_{3\text{-in.}}$	coefficient for 3 in. floor-to-centerline spacing
L	length of test article impacted by jet
m	model
off_{cyl}	vertical distance from test article base to nozzle centerline
p	prototype
r	radial distance from jet centerline
Re	Reynolds number
r_{jet}	jet radius
TI	free stream turbulence
U	jet velocity
$U_c(x)$	centerline velocity of free jet
$U_{max,m}$	maximum model jet velocity for a near-floor jet
U_o	nozzle exit velocity
U_{om}	model-scale jet exit velocity
$U_o d_o$	nozzle discharge parameter
x	distance from jet nozzle to test article centerline
x/d_o	normalized distance from nozzle
y	transverse location
z	vertical elevation

Greek Letters

ϵ/d_{cyl}	surface roughness
θ	jet half angle of expansion
μ	viscosity
ν	kinematic viscosity
ρ	fluid density

REFERENCES

1. Donald, M. B., and H. Singer. 1959. "Entrainment in Turbulent Fluid Jets." Transactions Institution of Chemical Engineers 37: 255-267.

2. Rouse, H. 1958. Advanced Mechanics of Fluids. John Wiley & Sons, Inc., New York, New York.

3. Roberson, J. A., and C. T. Crowe. 1975. Engineering Fluid Mechanics. Houghton Mifflin Company, Boston, Massachusetts.

4. Cheremisinoff, N. P. (ed.). 1986. Encyclopedia of Fluid Mechanics, Vol. 1. Gulf Publishing Company, Houston, Texas.

5. Bamberger, J. A., J. M. Bates, and E. D. Waters. 1990. Final Report: Experimental Characterization of Jet Static Forces Impacting Waste Tank Components. PNL-7394, Pacific Northwest Laboratory, Richland, Washington.

END

DATE FILMED

6 / 30 / 92